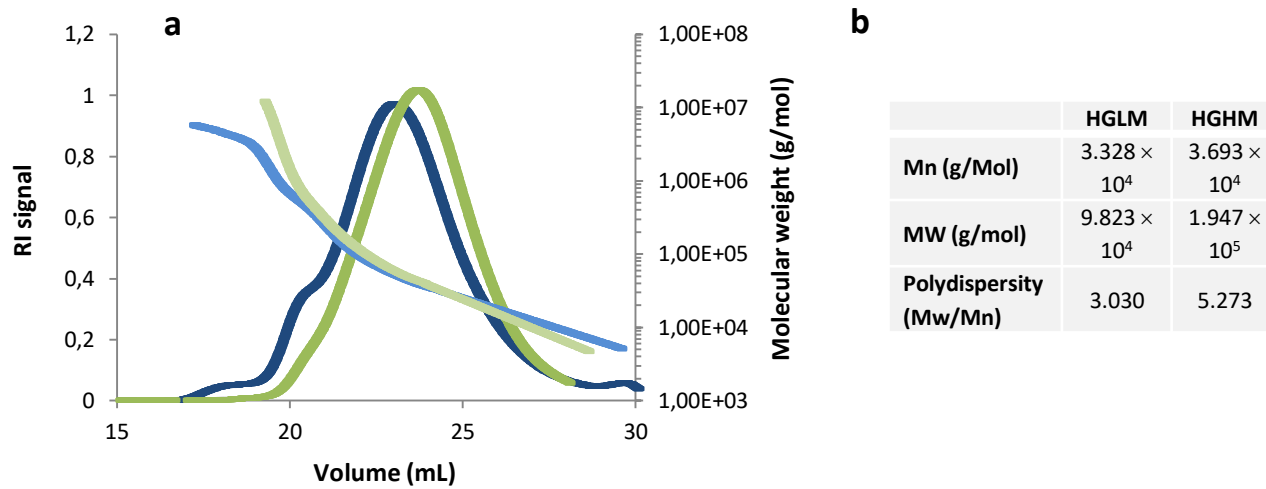
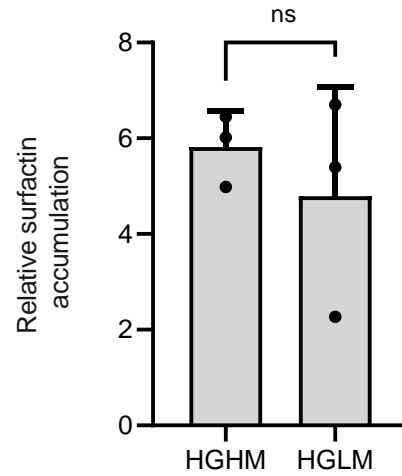


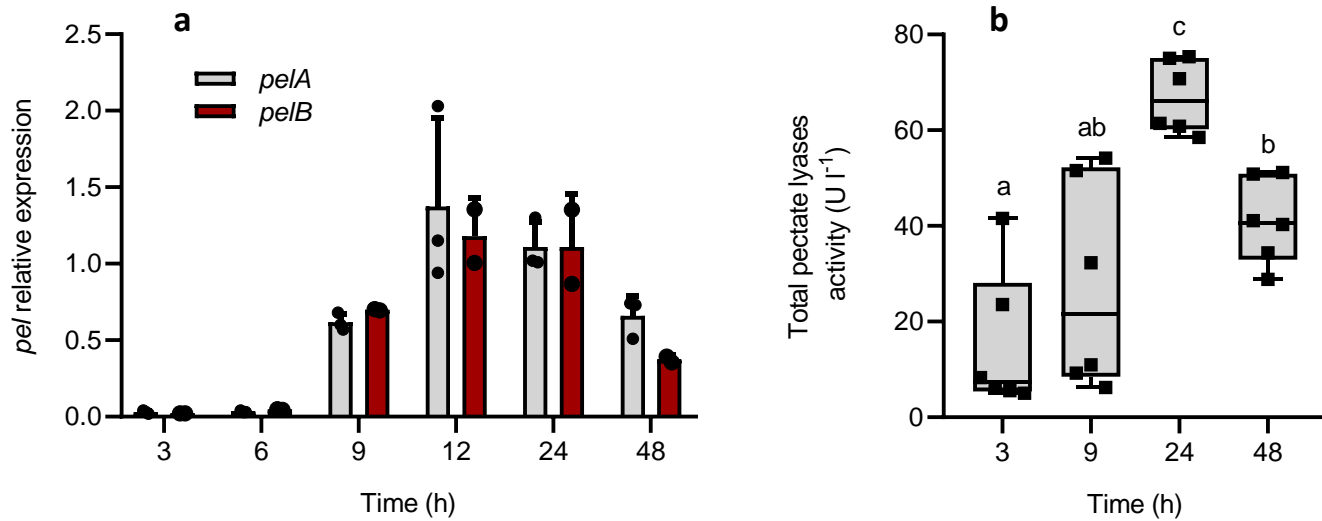
Supplementary Fig. 1: Pectin polysaccharide composition and structure. **a** Sugar composition analysis of crude pectin (cPec) extracted from tobacco roots. Composition is expressed as Molar Ratio percentage (Molar %) for each fraction. Galacturonic acid (orange) constituting the pectin backbone (**b** for schematization) is the main sugar of the cPec fraction. Other minor sugars (rhamnose, galactose, arabinose...) are typically found in the pectin side chains (Mohnen et al. 2008, **b**). **b** Schematization of pectin structure. Homogalacturonan (HG) contains an assembly of at least 100 galacturonic acid (GalA) residues that can be acetyl or methyl esterified. Rhamnogalacturonan I (RGI) is constituted by a succession of GalA-Rha dimers, each one containing an alternance of rhamnosyl and galacturonic acid units. The Rha unit can be branched with variable neutral sugar side chains including essentially galactosyl and/or arabinosyl units. Rhamnogalacturonan II (RGII) structure is well conserved within the HG polymer. RGII englobes 9 GalA units substituted by four side chains with complex sugars, including apiose, DHA, aceric acid and KDO, neutral sugars like, rhamnose, galactose, arabinose, xylose, and fucose or also organic acids such as galacturonic and glucuronic acid. RGII can also complex with Bore allowing a crosslink between two HG molecules.



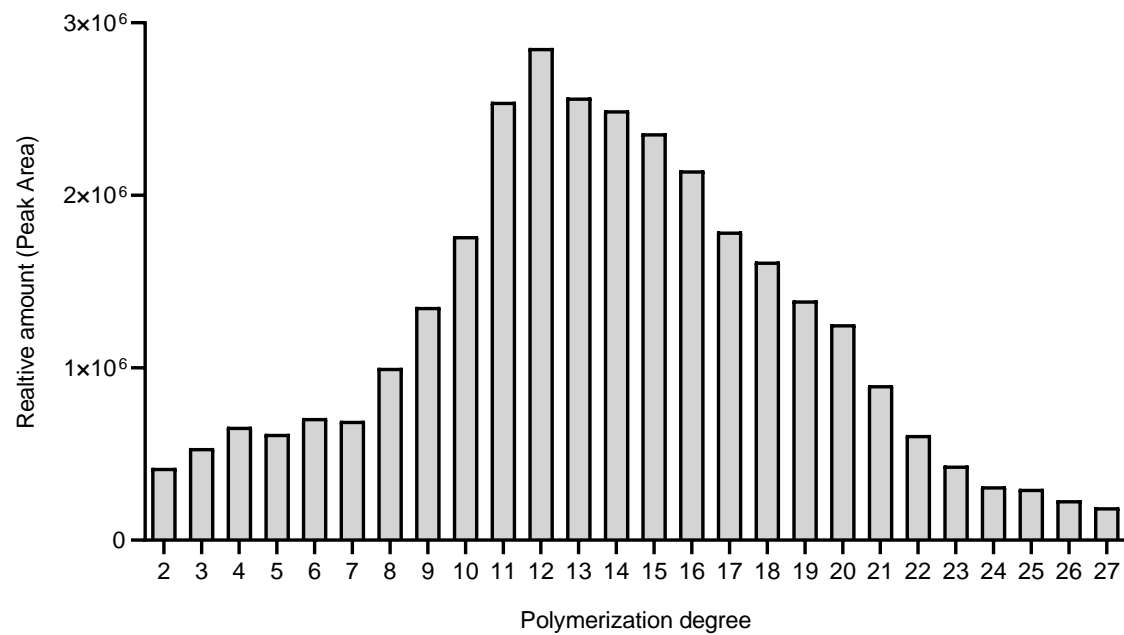
Supplementary Fig. 2: SEC-MALLS characterization of high and low methylated homogalacturonan
a SEC-MALLS profile of high (blue) and low (green) methylated homogalacturonan. Light curves represent the molecular weight distribution, dark curves represent the RI signal. **b** SEC-MALLS results. Mn: number average molecular weight, Mw : weight-average molecular weight, and polydispersity values (Mw/Mn).



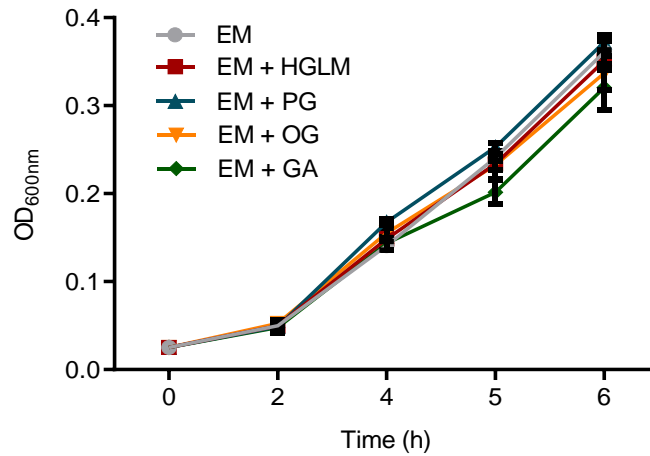
Supplementary Fig. 3: Relative surfactin accumulation by GA1 cells at early growth phase ($OD_{600}=0.2$) after addition of low (HGLM) or high (HGHM) methyl-esterified HG. Means \pm std err. from three biological replicates of one representative experiment are shown ns= non significant.



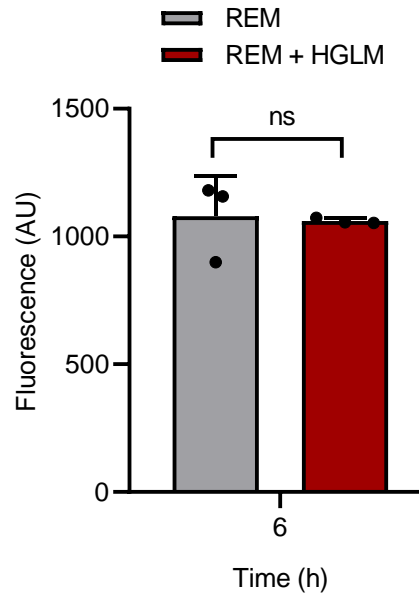
Supplementary Fig. 4: Characterization of *pel* expression and pectate lyase activity in GA1. **a** Evolution of *pelA* (grey) and *pelB* (red) expression pattern (n=3) For each time point, means \pm std err. from three biological replicates of one representative experiment are shown **b** Evolution of global pectate lyase activity in a 48h time course experiment. Means \pm std err. from three biological replicates of two experiments are shown. Significate differences are indicated by different letters (n=6).



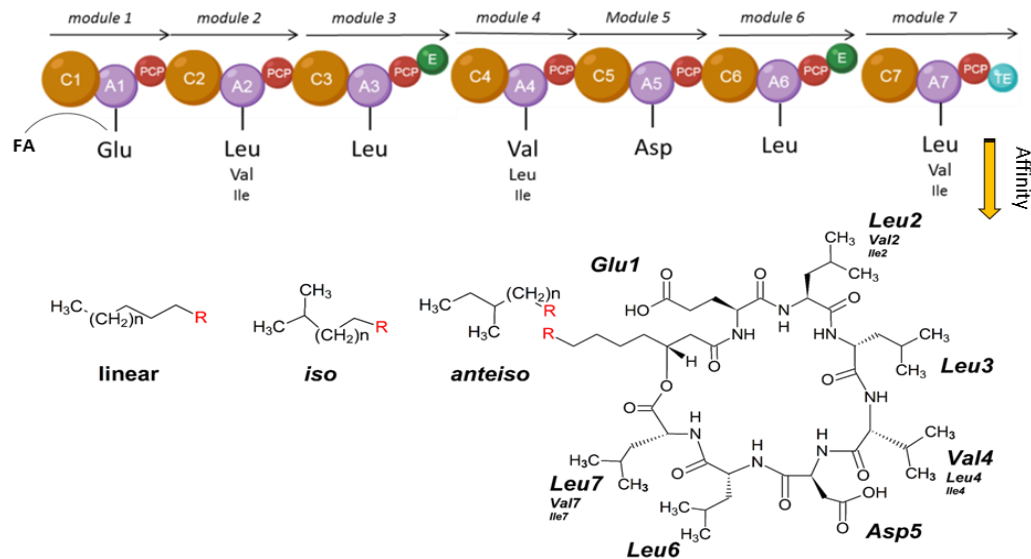
Supplementary Fig. 5: Characterization of oligogalacturonides (OG) polymerization degree by HILIC-QTOF



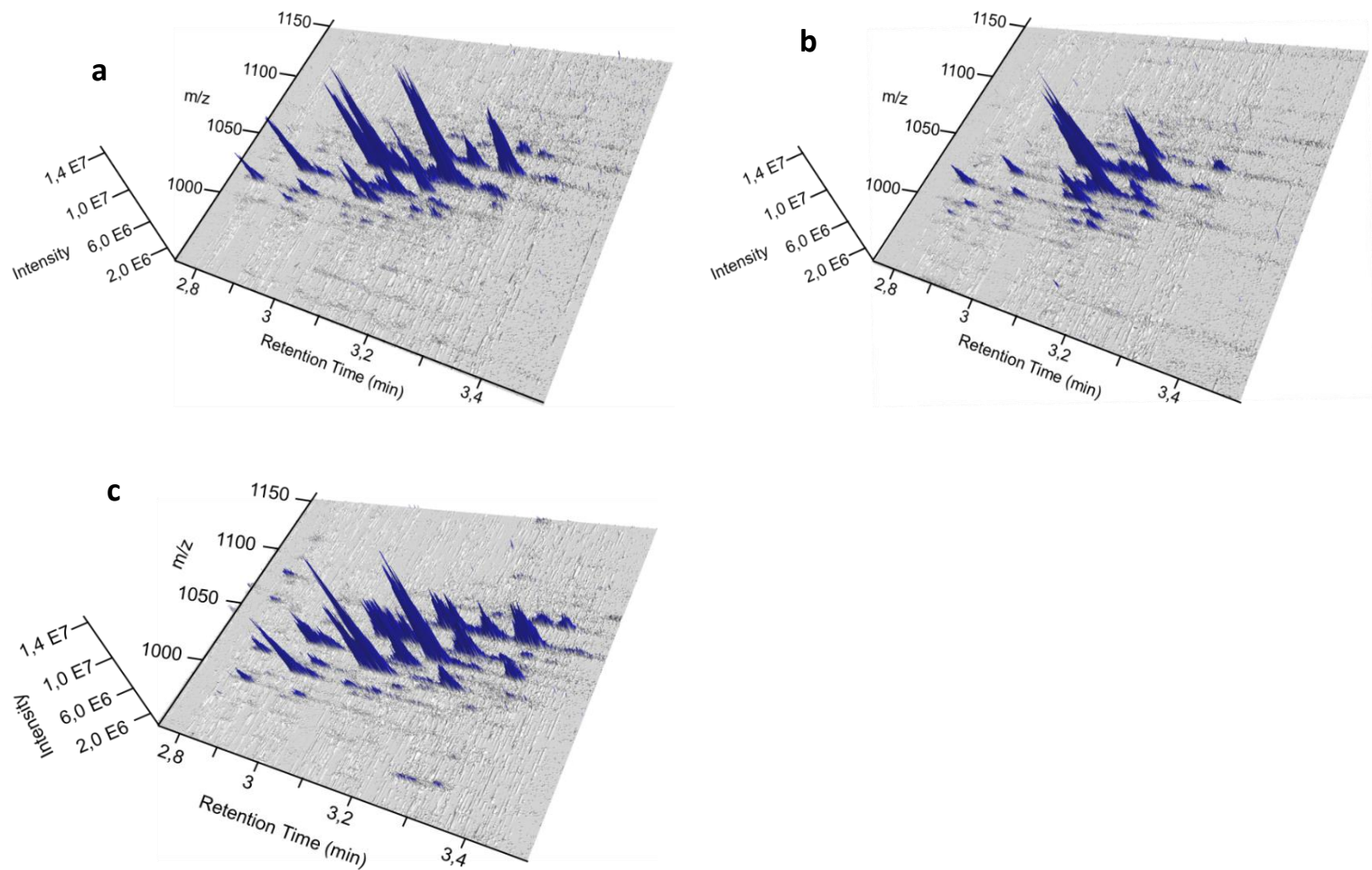
Supplementary Fig. 6: GA1 early growth curves. Liquid culture was performed in EM medium alone (grey) or supplemented with homogalacturonan (HG, red), polygalacturonides (PG, blue), oligogalacturonides (OG, orange) or galacturonic acid (GA, green). Error bars indicate standard error (n=3).



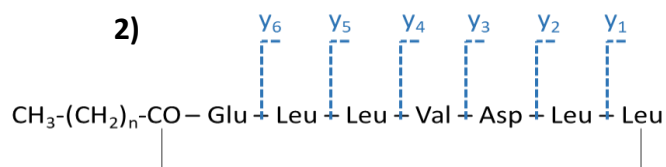
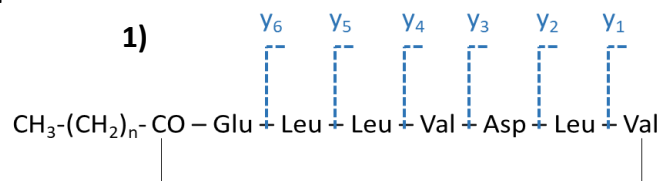
Supplementary Fig. 7: Surfactin expression measured by fluorescence in the GA1 *P_{srfAp}::gfp* reporter strain at early exponential phase in REM medium (grey bars) compared to REM medium supplemented with HGLM (red bars). Means \pm std err. from three biological replicates of one representative experiment are shown ns = non significant.



Supplementary Fig. 8: Representation of the NRPS machinery leading to the assembly of the surfactin molecule. This mega-enzyme is organized in 7 functional units called modules which are each responsible for the incorporation of one amino acid building block into the growing peptide chain. Each module is subdivided into different domains including an adenylation (A, violet circle) and a peptidyl carrier protein (PCP, red circle) catalyzing the peptide initiation, and one condensation domain (C, brown circle) responsible for peptide elongation. The termination of the peptide synthesis is performed by a thioesterase domain (TE, blue circle) in the last module. Modules 3 and 6 also possess an epimerization domain (E, green circle). Surfactin molecule contains a 7 amino acids chain structured as follow: L-Glu – L-Leu – D-Leu – L-Val – L-Asp – D-Leu – L-Leu. In some specific variants, Leu in position 2 and/or 7 can be substituted by a Val and more rarely by an Ile, and inversely, Val in position 4 can be substituted by a Leu and also more rarely by an Ile. In addition to the amino acid chain variability, multiple homologs with the same peptidic core but differences in terms of fatty acid chain length (C_{12} to C_{17}) or isomerisation of this latter (iso, anteiso or linear configuration) can also be produced.



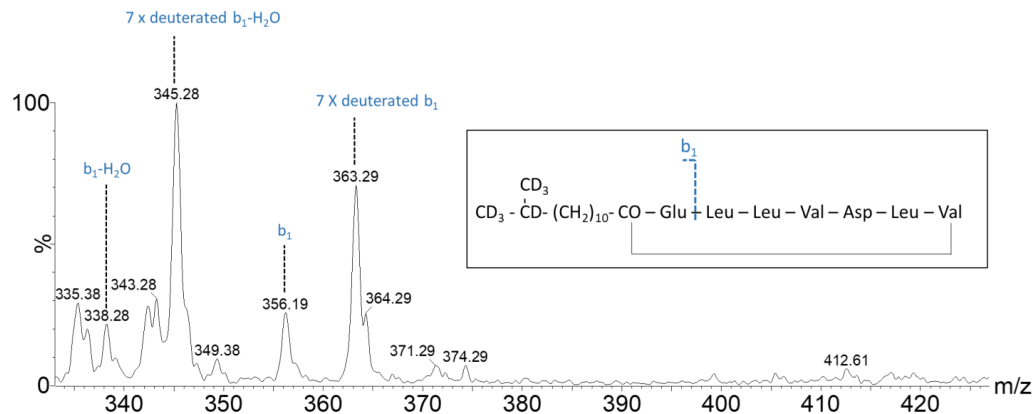
Supplementary Fig. 9: UPLC-MS 3D representation of *B. velezensis* surfactin pattern diversity produced in REM medium (a), in natural root exudates (b), or in planta (c). The X axis indicates the retention time (min), the Y axis the mass to charge ratio (m/z) and the Z axis the peak intensity (AU). Each blue peak represents a surfactin homologue.

a

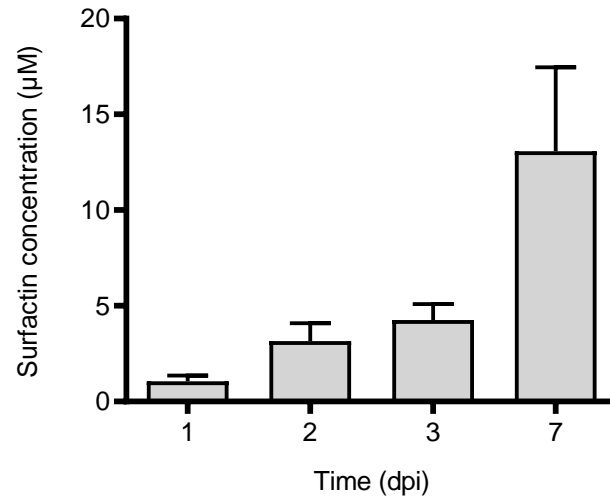
Supplementary Fig. 10: HR-MSMS analyses. a Schematic representation of surfactin fragmentation. **1)** surfactin Leu₇; **2)** surfactin Val₇ **b** List and mass error of detected y-ions after fragmentation of surfactins produced in EM for C13 to C15 Leu⁷ and Val⁷ surfactins.

b

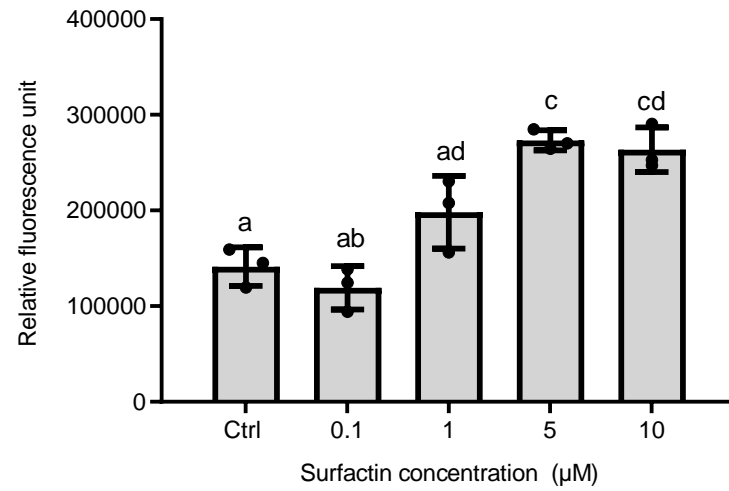
Fragment Ion ID	Fragment ion Formula	Fragment m/z	Detected Mass Error (ppm)
C13 Leu⁷ surfactin (precursor ion : m/z = 1008,659112)			
y6	C33H61N6O9	685,449454	-0,3
y5	C27H50N5O8	572,36539	-1,7
y4	C21H39N4O7	459,281326	0,1
y3	C16H30N3O6	360,212912	-2,5
y2	C12H25N2O3	245,185969	-1,1
y1	C6H14NO2	132,101905	-0,2
C13 Val⁷ surfactin (precursor ion : m/z = 994,643462)			
y6	C32H59N6O9	671,433804	1,2
y5	C26H48N5O8	558,34974	#N/A
y4	C20H3 N4O7	445,265676	-2,7
y3	C15H28N3O6	346,197262	-1,1
y2	C11H23N2O3	231,170319	0,2
y1	C5H12NO2	118,086255	1,4
C14 Leu⁷ surfactin (precursor ion : m/z = 1022,674762)			
y6	C33H61N6O9	685,449454	0,3
y5	C27H50N5O8	572,36539	-1,9
y4	C21H39N4O7	459,281326	1,5
y3	C16H30N3O6	360,212912	0,9
y2	C12H25N2O3	245,185969	0,7
y1	C6H14NO2	132,101905	1,5
C14 Val⁷ surfactin (precursor ion : m/z = 1008,659112)			
y6	C32H59N6O9	671,433804	0,2
y5	C26H48N5O8	558,34974	-0,8
y4	C20H37N4O7	445,265676	1,9
y3	C15H28N3O6	346,197262	1,5
y2	C11H23N2O3	231,170319	-1,5
y1	C5H12NO2	118,086255	1,7
C15 Leu⁷ surfactin (precursor ion : m/z = 1036,690412)			
y6	C33H61N6O9	685,449454	-0,3
y5	C27H50N5O8	572,36539	-0,9
y4	C21H39N4O7	459,281326	-0,9
y3	C16H30N3O6	360,212912	-1,5
y2	C12H25N2O3	245,185969	-1,3
y1	C6H14NO2	132,101905	0,9
C15 Val⁷ surfactin (precursor ion : m/z = 1022,675762)			
y6	C32H59N6O9	671,433804	0,6
y5	C26H48N5O8	558,34974	-0,6
y4	C20H3 N4O7	445,265676	-0,3
y3	C15H28N3O6	346,197262	0,9
y2	C11H23N2O3	231,170319	#N/A
y1	C5H12NO2	118,086255	3,4



Supplementary Fig. 11: Impact of medium supplementation with deuterated L-Val-d⁸ on *B. velezensis* surfactome. Precursor feeding with 8 time deuterated valine will result in a mass increment of 7 mass unit in iso-even fatty acid (i.e. iso-C14; see insert) due the loss of α -deuterium during the transamination step ¹. Fragmentation of iso-C14 surfactin show a high proportion of deuterated b₁ and b₁-H₂O fragment (m/z = 363 and 345 respectively). A small proportion of non-deuterated b₁ and b₁-H₂O is also visible in the spectrum (m/z = 356 and m/z = 338 respectively).



Supplementary Fig. 12: Estimated surfactin concentration surrounding the rhizoplan in a solid matrix. Surfactin was quantified based on the amounts measured by UPLC-MS in three extracts (mean \pm sd), each prepared from 3 roots and surrounding gelified medium from 3 individual plantlets. Surfactin concentration (μM) was calculated based on the mean value.



Supplementary Fig. 13: Impact of surfactin on cytosolic ROS accumulation in tomato. Means \pm std err. from three biological replicates of one representative experiment are shown. Significant difference between each condition is indicated by different letters. P-value < 0.05